

Gene expression

SOMDE: a scalable method for identifying spatially variable genes with self-organizing map

Minsheng Hao  1, Kui Hua  1,* and Xuegong Zhang  1,2,*

¹MOE Key Laboratory of Bioinformatics and Bioinformatics Division, BNRIST, Department of Automation, Tsinghua University, Beijing 100084, China and ²School of Life Sciences, Center for Synthetic and Systems Biology, Tsinghua University, Beijing 100084, China

*To whom correspondence should be addressed.

Associate Editor: Peter Robinson

Received on December 12, 2020; revised on May 22, 2021; editorial decision on June 22, 2021; accepted on June 23, 2021

Abstract

Motivation: Recent developments of spatial transcriptomic sequencing technologies provide powerful tools for understanding cells in the physical context of tissue microenvironments. A fundamental task in spatial gene expression analysis is to identify genes with spatially variable expression patterns, or spatially variable genes (SVgenes). Several computational methods have been developed for this task. Their high computational complexity limited their scalability to the latest and future large-scale spatial expression data.

Results: We present SOMDE, an efficient method for identifying SVgenes in large-scale spatial expression data. SOMDE uses self-organizing map to cluster neighboring cells into nodes, and then uses a Gaussian process to fit the node-level spatial gene expression to identify SVgenes. Experiments show that SOMDE is about 5–50 times faster than existing methods with comparable results. The adjustable resolution of SOMDE makes it the only method that can give results in ~5 min in large datasets of more than 20 000 sequencing sites. SOMDE is available as a python package on PyPI at <https://pypi.org/project/somde> free for academic use.

Availability and implementation: SOMDE is available for download from PyPI, and the source code is openly available from the Github repository <https://github.com/XuegongLab/somde>.

Contact: zhangxg@tsinghua.edu.cn or stevenhuakui@gmail.com

Supplementary information: [Supplementary data](#) are available at *Bioinformatics* online.

1 Introduction

The spatial location of cells in tissues and corresponding gene expression profiles play pivotal roles in the study of tissue mechanism and tumor immune microenvironment. Spatial transcriptomics sequencing technologies provide gene expression profiles with spatial information, filling the gap between high throughput transcriptomics and their spatial context.

Since the publication of Spatial Transcriptomic (ST) (Ståhl *et al.*, 2016), the number of measured spatial data sites in one sample has increased from a few hundred to tens of thousands. Targeted in-situ sequencing technologies such as seqFISH+ (Eng *et al.*, 2019) and MERFISH (Moffitt *et al.*, 2018) capture single-cell level transcripts under the camera field of view (FOV). They splice multiple adjacent FOV results to form datasets with a large number of cells. Advanced Spatial Transcriptomic methods such as Slide-seq (Rodrigues *et al.*, 2019) and 10X Visium (the commercial version of original ST) can sequence 5000–25 000 spatial data sites with a resolution of 10 and 55 μm , respectively. It is foreseeable that the scale of spatial transcriptomic data will increase quickly.

Spatial transcriptomic data provides gene expressions with physical location information. Spatial variations of gene expression reflect the cell-cell interaction relationship (Dries *et al.*, 2021) and help determine compositions of cell types that perform spatial specific functions. Identifying spatially variable genes (SVgenes) is the basic task for spatial transcriptomic data analysis. Compared with previous tasks of identifying highly variable genes (HVG) from gene expression profiles, SVgene identification needs to consider not only variations between cells but also the spatial significance of gene expression.

Several methods such as Trendsseek (Edsgård *et al.*, 2018), SpatialDE (Svensson *et al.*, 2018), SPARK (Sun *et al.*, 2020), scGCO (Zhang *et al.*, 2018), Giotto (Dries *et al.*, 2021) have been proposed for identifying SVgenes in recent years. Despite the great success of those methods in low-throughput spatial transcriptomic data, the high computational complexity hinders their application in large-scale datasets. For example, when the number of sites exceeds 20 000, Trendsseek, SpatialDE and SPARK will require at least 1000 min to get results (Sun *et al.*, 2020).

To better cope with the growth of spatial transcriptomic data sizes, we present SOMDE, a scalable method to identify

SVgenes with high computational efficiency. SOMDE uses the self-organizing map (SOM) neural network and Gaussian process to model spatial data. We conducted a series of experiments on both synthetic and real datasets which are obtained by two scalable protocols. Results showed that SOMDE gave similar SVgenes as existing methods, but in much less time with enhanced spatial pattern visualization. The adjustable number of nodes enables SOMDE to get results in large-scale datasets with more than 20 000 sites in only 5 min. We have developed SOMDE as a python package available on PyPI at <https://pypi.org/project/somde> free for academic use.

2 Materials and methods

2.1 Overview of SOMDE

The transcript expression of SVgene is highly correlated with the spatial location and exhibits clustered, periodic or other patterns in space. Most of the published methods (Trendsseek, SpatialDE and SPARK) characterize the gene expression patterns based on the statistical spatial correlation models. The size of covariance matrices in their model grows quadratically as the number of spatial sites increases, and therefore both time and memory consumption are needed to be optimized. Other methods (scGCO and Giotto) use gene expression binarization and non-statistical modeling to improve computational efficiency, but their scalability is still limited on the large-scale data.

The key idea of SOMDE is to construct a condensed representation of spatial transcriptomic data that both preserves the information of SVgenes and reduces the downstream computational complexity. We use the SOM neural network to adaptively integrate neighboring data into different nodes, and then identify SVgenes based on the node-level spatial location and gene expression information using a modified Gaussian process (Fig. 1).

2.1.1 Data site integration

The spatial expression of SVgenes usually has certain continuity. A proper strategy of data site integration should preserve the spatial expression patterns of SVgenes and the topological structure of data sites. SOM meets both the requirements. SOMDE first adopts SOM to integrate spatial data sites into nodes and then assigns the gene expression profile of each node.

SOM is an unsupervised neural network first proposed by Kohonen (Kohonen, 1984). It is an $N \times N$ array of neurons (nodes) arranged in a grid on the 2D plane. The neurons are connected to the input vector with trainable weights. The weights of neighboring nodes undergo competitive learning during the training phase so that a properly trained SOM will show the ‘self-organizing’ property that preserves the topological relations and relative densities of the samples in the original input space (Kohonen, 1984; Zhang and Li, 1993). We apply SOM on the spatial gene expression data by using the 2D coordinates x of each data site as the input to the nodes. In this way, the trained SOM forms a condensed map that uses the node weights as a down-sampling representation of the original spatial information (Uriarte *et al.*, 2005).

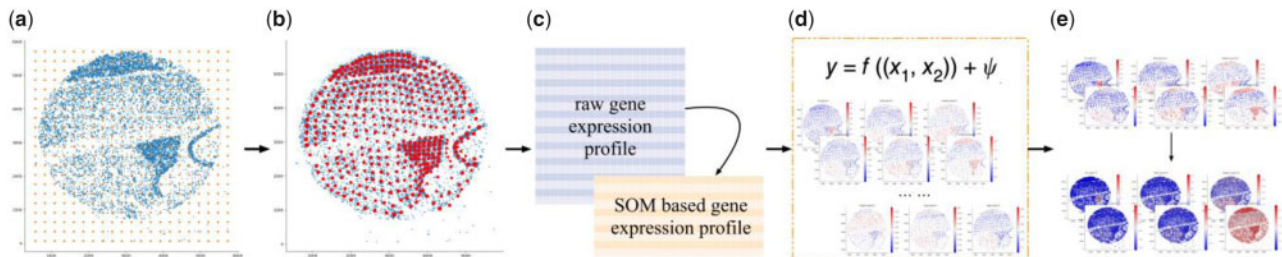


Fig. 1. A schematic overview of SOMDE. (a) SOMDE initializes a self-organizing map (SOM) on the tissue spatial domain. (b) By training the SOM with data site locations, SOMDE condenses the original data site coordinates (blue spots) into SOM node coordinates (red spots). (c) Then SOMDE converts the original spatial gene expression to node-level gene meta-expression profiles. (d) SOMDE models the condensed representation of the original spatial transcriptome data with a modified Gaussian process. The variability of the gene expression y is decomposed into two parts, a spatial part $f(x_1, x_2)$ that can be explained by the location of cells, and a non-spatial part ψ for the rest of the variability. (e) SOMDE identifies genes with high spatial variability expression patterns as SVgenes, and maps node-level expression patterns of SVgenes to their original expression patterns

Specifically, we use a square SOM with N rows and N columns of nodes to learn the condensed representation. The size N can be determined according to the following formula:

$$N^2 \times k = C \quad (1)$$

where C is a constant representing the total number of data sites, and k is the model parameter called neighbor number, which denotes the expected average number of original data sites each SOM node represents. This parameter controls how condensed the learned SOM is. A larger k means higher condensation.

We initialize the value and dimension of the SOM node weights $M = (m_1, m_2, \dots, m_{N \times N})$ with the uniform grid coordinates on the tissue spatial domain (Supplementary Materials). An example of the initialized SOM node weight is plotted in orange in Figure 1a. After initialization, SOM adjusts the weight of each node toward the tissue spatial topology through a repetitive training process using all spatial coordinates $X = (x_1, x_2, \dots, x_C)$ as training samples. We applied the batch SOM training algorithm (Wittek *et al.*, 2017) in SOMDE. One spatial coordinate x is fed to SOM in one step and a cycle of all spatial coordinates is called one epoch. All node weights are parallelly updated once after one epoch. Multiple epochs are conducted during the whole training process. It takes less than 1 s to train a SOM in a dataset of 20 000 sites by taking this parallel implementation. The further elaboration of the training algorithm is in the Supplementary Material.

After training, each data site maps to a unique SOM node. Each SOM node represents the group of sites that mapped to it. Node weights in the learned SOM can be treated as new spatial coordinates for the data sites. The new spatial locations $\tilde{X} = (\tilde{x}_1, \tilde{x}_2, \dots, \tilde{x}_{N \times N})$ compose the sparse topology of the original data, as shown in red in Figure 1b. To represent the expression of a gene on the condensed map, we define the gene ‘meta-expression’ at a SOM node as the linear combination of the max value and average value of the gene expression in the group of sites that the node represents. The reason for not using average value as meta-expression is due to the high sparsity in large-scale data that could bias the result. Suppose x_{S1}, x_{S2}, \dots are a set of neighboring data sites mapped to a SOM node (i, j) , the meta-expression $\tilde{y}_{i,j}$ of one gene at this node is

$$\tilde{y}_{i,j} = \gamma \cdot \max(y_{S1}, y_{S2}, \dots) + (1 - \gamma) \cdot \text{avg}(y_{S1}, y_{S2}, \dots) \quad (2)$$

where y_{Si} is the expression value of the gene at the data site x_{Si} . The combination ratio γ balances the local maximum and mean gene expression. We use $\gamma = 0.5$ as the default in current experiments.

With this mapping and data integration for all gene and all data sites, we obtain the condensed representation of the original spatial transcriptome data by the meta-expression map in the SOM plane that best preserves the original topological and expression information. The resolution of this condensed spatial transcriptomic map can be adjusted by the parameter k .

2.1.2 Spatial expression variability identification

The second step is identifying gene spatial expression variability with the condensed spatial transcriptomic map. We consider one gene meta-expression at one time and introduce an adjusted

Gaussian process H_G in SOMDE to model the spatial correlation. Model H_G decomposes the expression variability into spatial and non-spatial components:

$$p(\tilde{y} | H_G, \tilde{X}, \Theta) = \mathcal{N}(\tilde{y} | \mu \cdot 1, \sigma_s^2 \cdot \Sigma_{k(\tilde{x}, \tilde{x}' | \theta)} + \delta \cdot I) \quad (3)$$

where \tilde{y} denotes one gene meta-expression in the SOM plane and \tilde{X} denotes SOM nodes locations. $\delta \cdot I$ indicates the non-spatial variance given by Gaussian distributed noise in all observed gene meta-expression. $\Sigma_{k(\tilde{x}, \tilde{x}' | \theta)}$ captures the spatial variation by using a selected kernel function $k(\cdot)$. Here \tilde{x} and \tilde{x}' represent the locations of any two SOM nodes. The kernel function $k(\cdot)$ introduces the spatial correlation between them. We applied a squared exponential (Gaussian) kernel in our model, since it can capture any spatial pattern (Svensson et al., 2018). By taking SOM nodes as the basic units, the covariance matrix is reduced to $1/k^2$ of the original matrix compared with previous statistical methods. We generated 10 Gaussian models with different length scales in SOMDE and choose the one with the highest log-likelihood ratio value. We used Θ to denote the parameters that need to be optimized, including the mean value μ , spatial signal variance σ_s^2 and noise variance δ . We applied gradient optimization to estimate these parameters.

The two separated variances allow us to get the fraction of spatial variation (FSV) in total variance by calculating the proportion of $\sigma_s^2 g$ in $\sigma_s^2 g + \delta$, g is the variance calculated from $\Sigma_{k(\tilde{x}, \tilde{x}' | \theta)}$ using the Gower's transformation (Svensson et al., 2018). Compared with the original Gaussian process model, model H_G assumes one gene meta-expression at all spatial locations has the same mean value μ so that the non-spatial variance cannot be regressed out. Thus the maximum likelihood value of H_G mainly depends on spatial variance.

We use a similar log likelihood ratio test as SpatialDE to determine the statistical significance of each gene's spatial expression variability. Consider a Gaussian model H_0 without the spatial covariance term:

$$p(\tilde{y} | H_0, \tilde{X}, \theta) = \mathcal{N}(\tilde{y} | \mu \cdot 1, \delta \cdot I) \quad (4)$$

where μ and δ represent the mean value and noise variance, respectively. The log-ratio test between H_0 and H_G reflects the significance of the spatial variance. And the P -value can be estimated by assuming the log-likelihood ratios (LLR) are χ^2 distributed with one degree of freedom. SOMDE takes the LLR value as the spatial variability score for each gene and ranks them accordingly from high to low.

The top SVgenes ranks given by SOMDE at different resolutions may be different. To get a unified result, we propose a k -free solution called combined-SOMDE (cSOMDE) to merge all results. For each gene, cSOMDE takes the geometric mean of ranking results given by SOMDE with three different k as the final rank. This strategy considers the spatial variability of the same gene expression at different reduced resolutions.

SOMDE is implemented in Python and uses somoclu V1.7.5 for multi-thread building SOM. We choose SpatialDE V1.1.0, scGCO V1.1.1, SPARK V1.1.0 and Giotto V0.3.1 as representatives of statistical methods and non-statistical methods for comparison. All experiments are based on 16 AMD Ryzen 7 1700X Eight-Core Processors.

3 Results

3.1 Datasets and experiments design

We conducted a series of experiments on simulated data and real data to study the performance of SOMDE. The simulation data were used to evaluate the method performance under different settings of signal-to-noise ratios (SNRs) and dropout rates. On the real data where ground truth is not available, we studied the numbers of

SVgenes and examples of the identified SVgenes in comparison with other methods to illustrate the performance of the SOMDE.

3.1.1 Experiments on simulation data

We adopted the Gaussian process-based model (Equation 3) to synthesize a series of simulation data. The simulation data are based on 9650 spatial locations (data sites) collected from the Slide-seq near Hippocampus (nHipp) data (Rodrigues et al., 2019). We generated 100 SVgenes and 900 genes with no spatial variation (non-SVgenes) for each simulation. To mimic the real gene spatial expression data, we added Gaussian noise and dropout events to the simulation data. For a quantitative evaluation, we define the spatial pattern strength, or signal strength as the standard deviation of the expression data, the noise level as the standard deviation parameter in the Gaussian noise model, and the dropout rate as the proportion of data sites that we force the expression value to be 0 among all data sites. We use different settings of these parameters in each simulation and organize the experiments in terms of signal-to-noise ratio (SNR, defined as the ratio of signal strength to the noise level) and the dropout rate. Details of the generation procedure can be found in the Supplementary Materials.

We conducted three sets of experiments to systematically evaluate the performance of SOMDE. The first set of experiments aims to examine the methods under different SNRs when all information is observed, i.e. without dropout; To evaluate the performance when different combinations of SNRs and dropout rates exist in the data, we introduced the same dropout rate to data with different SNRs in the second set of experiments, and changed the dropout rate in data with the same SNR in the last set of experiments.

Specifically, the parameter settings (signal strength, noise level) in the first set were (0.1, 0.1), (0.15, 0.1), (0.2, 0.1), (0.1, 0.35), (0.15, 0.35) and (0.2, 0.35). We adopted the same settings of SNR in the second set of experiments as the first set, but added a dropout rate of 0.2 to each simulation. In the third set of experiments, we used a fixed setting of the signal strength and noise level (0.15, 0.1), with a varying dropout rate ranging from 0 to 0.9. It should be noted that some extreme cases (i.e. excessively high dropout rate or low SNR) covered by our simulation may not appear in real data but are suitable for testing the performance of the methods.

We compared SOMDE with SpatialDE and scGCO. SPARK is not included because of its incapability of getting a result on most simulations. We compared the ability of different methods to distinguish SVgenes from non-SV genes. Specifically, we regraded SVgenes as positive cases and non-SVgenes as negative cases. For each method, we used its reported statistic (i.e. log-likelihood ratios for SOMDE and SpatialDE, P -value for scGCO) to classify genes. We drew the ROC and FDR-power curves of the three methods on each simulation data. The ROC curve is used to evaluate the general performance of different methods, and the FDR-Power curve can better reflect the method's ability to control false positive samples.

3.1.2 Experiments on the real data

We tested SOMDE on six large-scale real datasets: 10X Visium Brain, Visium Breast Cancer, Hippocampus (Hipp), near Hippocampus (nHipp), Liver and Kidney. These datasets are produced by two scalable spatial sequencing protocols: The Brain and Breast Cancer datasets are obtained by 10X Visium, and the other four datasets are obtained by Slide-seq (Rodrigues et al., 2019).

Table 1. Overview of datasets used in our experiments

Protocol	Tissue	Gene number	Site number
10X Visium	Brain	14 414	2693
10X Visium	Breast Cancer	16 317	3987
Slide-seq	Hippocampus	3235	12 218
Slide-seq	near Hippocampus	2555	9650
Slide-seq	Liver	2238	17 454
Slide-seq	Kidney	4650	22 860

Brief descriptions of these datasets are shown in Table 1. The spatial resolutions of the 10X Visium and Slide-seq protocol are 55 and 10 μm , respectively. Although these data are not at the single-cell level, the measured gene expressions are highly correlated with spatial locations. The large gene and data site number are suitable for verifying the computational efficiency of our SVgenes identification method.

Six datasets sequenced by two different protocols are used in our experiments. 10X data is downloaded from official 10X Genomics websites. The gene number and data site number indicate the scale of data after quality control.

We applied two pre-processing strategies to these datasets from two protocols. After getting the pre-filtered 10X Visium matrix, we filtered out genes whose total counts are less than 50 counts. Slide-seq datasets were downloaded from SpatialDB (Fan *et al.*, 2019) website and were also pre-filtered. For Slide-seq data, we kept all the genes but removed the data sites where the total counts are greater than a 4-fold change of the average total counts. Then we log-transformed the raw count matrix and regressed out the total counts of each data site. The regressed matrix is the final normalized matrix for downstream analysis.

We set the default neighbor number k to 20 for all these datasets. SOMDE takes spatial information and normalized gene expression matrix as input, gives the SVgene rank and tests the statistical significance of spatial variability with q -value. Genes with q -value smaller than 0.05 are identified as SVgenes. The SOMDE running time of all the above experiments has been recorded.

We further confirm the validity of identified SVgenes in nHipp and 10X Brain datasets from the biological and mathematical views. SOMDE was compared with four methods. They are SpatialDE that uses the modified Gaussian process directly for identification, SPARK that uses the GLSM model, scGCO that uses graph-cut and Giotto (SilhouetteRank) that introduces the silhouette score to rank binarized expressed genes. For the cSOMDE method, we set neighbor numbers $k = 5, 20, 40$ and $k = 4, 20, 40$ in 10X Brain and nHipp datasets, respectively. The default settings were used for all other methods.

We compared the number of identified SVgenes and the similarity of top-ranked genes reported by SOMDE, scGCO, SPARK, SpatialDE and cSOMDE. We visualized the SVgene expression patterns and used ISH datasets for further verification. We also tested the robustness of SOMDE under different hyper-parameters settings.

3.2 Simulation results

In the first set of experiments (Supplementary Fig. S1), we found that without dropout SpatialDE achieved a very high true positive rate (TPR). SOMDE gained a TPR of 0.8 with false positive rate (FPR) smaller than 0.05, regardless of the noise level being 0.1 or 0.35. After the signal strength was increased to 0.15, SOMDE got a similar performance as SpatialDE on both ROC and FDR-Power curves. Under all the settings, SOMDE outperformed scGCO which also focuses on the improvement of running efficiency, in terms of both power and the control of false positive (Supplementary Fig. S1).

We conducted the second set of experiments under the same SNR settings as the first ones, but added a dropout rate of 0.2 (Fig. 2, Supplementary Fig. S2). With the existence of dropout, the performance of all methods decreased (Fig. 2a–c). SOMDE still achieved a better performance than scGCO in all simulations. When the signal is weak (signal strength = 0.1), SOMDE is more sensitive to the increase of noise level compared to SpatialDE (Fig. 2a, b). This is caused by the combination of maximum and mean expression values to calculate the node-level meta expression in SOMDE. When the signal is extremely low, the meta-expression could be biased by the maximum values dominated by the noise, leading to a decreased power. However, the introduction of maximum value could enable SOMDE to capture weak signal patterns on sparse data. And a small increase in the signal strength would lead to comparable performance between SOMDE and SpatialDE, even when the noise level is high (Fig. 2c).

In the third set of experiments, we found that SOMDE outperforms other methods in addressing data sparsity (Fig. 2, Supplementary Fig. S3). SOMDE and SpatialDE had comparable

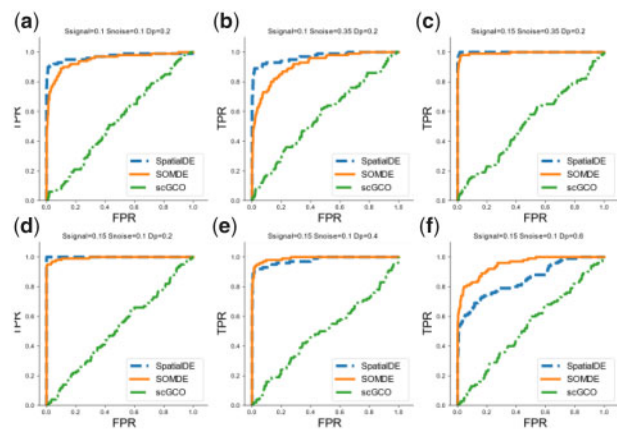


Fig. 2. Performance of different methods on simulation data with different signal-to-noise ratios (SNRs) and dropout rates. We used the ROC curve to show the performance of different methods on each simulation. The first row gives part of the results under different SNRs with a fixed dropout rate (experiment set 2). The second row shows part of the results when the dropout rate varies while SNR is fixed (experiment set 3). The specific parameter settings (signal strength, noise level, dropout rate) of the six results are (0.1, 0.1, 0.2), (0.1, 0.35, 0.2), (0.15, 0.35, 0.2), (0.15, 0.1, 0.2), (0.15, 0.1, 0.4), (0.15, 0.1, 0.6)

results with the dropout rate below 0.4 (Fig. 2d, e). SOMDE was more powerful than SpatialDE and scGCO across all FPR cutoffs with the dropout rate being 0.4–0.7 (Fig. 2e, f). When facing the high sparsity data (i.e. dropout rate = 0.8–0.9), all these methods failed to achieve a good performance. These results show that the data integration step in SOMDE not only boosts the computation but also makes it more robust to the data sparsity.

We also checked the P -value of non-SVgenes reported by SOMDE (Supplementary Fig. S4). Results showed that SOMDE provides good control of false positive and is insensitive to the selection of neighbor k.

3.3 Real data results

In the 10X Brain and Breast Cancer datasets, SOMDE found 5455 and 7356 SVgenes, respectively. In the Liver dataset, the SVgenes number is the smallest with only 164 genes. SOMDE found 699, 379, 522 SVgenes in Hipp, nHipp and Kidney datasets, respectively (Supplementary Table S1). *CRISP3*, *CPB1*, *CXCL14*, *COX6C* and *FCGRT* are the top 5 SVgenes identified by SOMDE in the 10X Breast Cancer dataset. The top 5 SVgenes in the 10X Brain dataset are *Sparc*, *Agt*, *Slc6a11*, *Tcf7l2* and *Nrgn*, respectively. *Nrgn* and *Tcf7l2* were also identified as the top 10 SVgenes in the nHipp and Hipp dataset. *Ttr* gene has the most spatial expression variability in both nHipp and Hipp datasets. In Liver and Kidney datasets, the top 5 SVgenes are *Mup17*, *Hpx*, *Mgst1*, *Ghl*, *Mup3* and *Napsa*, *Kap*, *Aadat*, *Mpv17l*, *Acadm*, respectively. All SVgene rank lists of these six datasets are available in the Supplementary Material.

From the results, we found that the different proportions of SVgene among datasets are more likely due to the biological characteristics of the tissue, rather than technical bias or different data sizes. In tissues with complex spatial correlated functions such as the whole adult mouse brain or hippocampus, the proportion of SVgenes is far greater than in the adult mouse kidney or liver tissues.

We plotted the top 50 SVgenes spatial expression patterns at the original resolution and node-level resolution in all datasets (Fig. 3, Supplementary Figs S5–S11) Each spot in the figure denotes one data site or one SOM node, and the color represents the relative expression values within one plot. The visualization results on the original data and condensed map show the similar topological structure of data sites and spatial gene expression patterns. We also checked the bottom 50 SVgenes on 10X Brain data (Supplementary Fig. S12). The spatial variabilities of these genes in the original resolution are less clearly compared to that of the top 50 ones and only a few are apparent to human eyes. However, most of these patterns

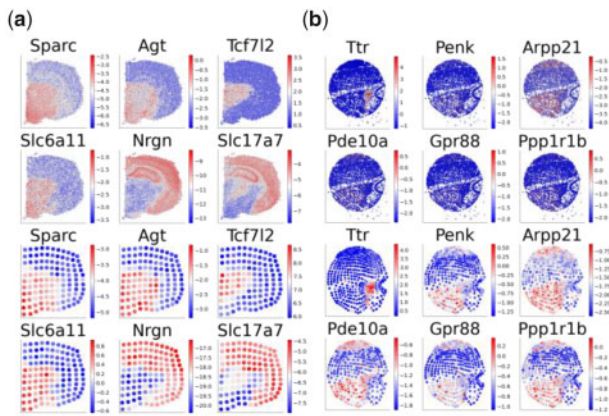


Fig. 3. The top 6 SVgenes found by SOMDE are visualized in original and SOM space. Top 6 SVgenes found in 10X Brain and nHipp datasets. Each subplot denotes one gene spatial expression pattern. Color implies the relative expression value within the plot. The first two rows and the last two rows are in the original space and SOM space, respectively

got enhanced in the condensed map of SOM (Supplementary Fig. S12).

The integration step of SOMDE improves the SNR of gene expressions on the Slide-seq nHipp dataset. *Pde10a*, *Gpr88* and *Ppp1r1b* genes (Fig. 3b) have low expression levels in the original tissue spatial domain so that it is hard to visualize their high spatial expression variability due to the noise and sparsity. On the condensed map, however, these genes show strong spatial patterns and variabilities. SOMDE successfully enhanced gene expressions via the combination of the maximum and average local expression. These results also suggest that the visible patterns shown on the original spatial domain may not be a golden standard for determining spatial variation.

We further analyze our SOMDE results on the Slide-seq nHipp and 10X Brain datasets to verify the identification results. We use the MGI database (Smith *et al.*, 2019) and Allen Brain Atlas (Lein *et al.*, 2007) as references to verify the genes' morphological function and spatial expression distribution. SVgenes identified by SOMDE showed clear spatial variation and well consistent with existing In Situ Hybridization (ISH) patterns of the same tissue (Supplementary Figs S13 and S14). For example, *Nrgn*, one of the top 5 SVgenes in the 10X Brain dataset, is responsible for the transcription of neurogranin protein that encodes transcription and signal synapse transduction. Expression patterns on both 10X Brain and ISH data reveal that *Nrgn* mainly expressed in the cerebral cortex and hippocampal formation (Supplementary Fig. S14). *Camk2n1*, another SVgene identified in the mouse brain, is responsible for the production of enzyme regulators and is highly expressed on the outer and posterior parts of the cerebral cortex on our condensed map. This spatial pattern is also cross-validated by the ISH data (Supplementary Fig. S14). Both *Nrgn* and *Camk2n1* play important roles in synaptic long-term potentiation (Ling *et al.*, 2011), and they have a similar spatial variability score and SVgene rank, suggesting our results are of potential biological interest.

We also confirm the validity of SOMDE from the mathematical view. Figure 4 shows the log-likelihood ratio (LLR) and the fraction of spatial variation (FSV) of all genes given by SOMDE in 10X Brain and nHipp datasets. Each spot denotes one gene and we highlight the spots of the top 5 SVgenes. The top 5 SVgenes in both datasets identified by our method have high FSV and LLR values. *Sparc* gene has the maximum LLR value corresponding to the most significant spatial patterns shown in Figure 3. For highly spatially variable genes, LLR and FSV values are positively correlated as expected. The gene spot distribution indicates most spatially variable genes have significant statistical values, which shows that the integration of spatial sites does not affect the identification of these gene variabilities.

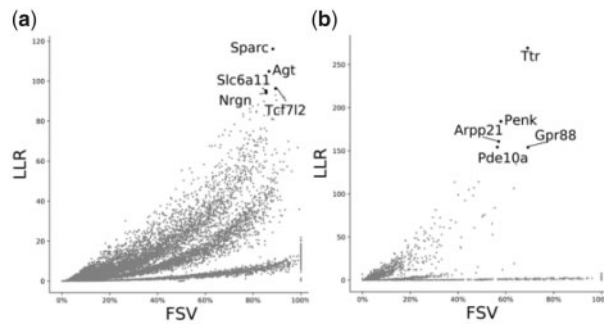


Fig. 4. Quantitative results of SOMDE in 10X Brain and nHipp datasets. The x-axis represents the fraction of variance explained by spatial variation (FSV), and the y-axis represents the log-likelihood ratio (LLR). The top 5 genes selected by our method are high on both indicators. (a) and (b) show results in brain datasets and nHipp datasets

Table 2. The running time of SOMDE in multiple datasets

Dataset	Gene number	Site number	Map	Time (s)
10X Brain	14 414	2693	11 × 11	247
10X Cancer	16 317	3987	19 × 19	354
Hipp	3235	12 218	24 × 24	56
nHipp	2555	9650	21 × 21	57
Liver	2238	17 454	29 × 29	58
Kidney	4650	22 860	33 × 33	147

Table 2 shows the running time of SOMDE in all six datasets. Running time refers to the total time from training self-organizing map to obtaining SVgene ranks and spatial variability scores. The adjustable map size guarantees the condensed maps are at the same resolution on different datasets. SOMDE gave all the results with no more than 5 min regardless of the gene and data site number. We can conclude that the condensed transcriptomic maps make the computational efficiency of SOMDE not limited by the dataset size.

The results of the SOMDE on different datasets with $k = 20$ ($k = 10$ on the 10X Cancer data). Although the running time is affected by the gene and sequencing site number, SOMDE gives results in less than 5 min in multiple datasets (some datasets even exceed 20 000 data sites), which shows the superiority of our method in terms of running time.

3.4 Comparison with existing methods on the real data

3.4.1 Gene ranking similarity

All methods get the results on the 10X Brain and nHipp data, except that SPARK failed to run on the nHipp data because of the data sparsity. These methods revealed similar judgments on the most spatially variable genes, regardless of their own criteria or principles (Fig. 5, Supplementary Figs S15, S16). In the 10X Brain dataset, SOMDE shared 4809, 5501, 3351 common SVgenes with SPARK, SpatialDE and scGCO (Fig. 5a), respectively. We also compared the similarity of all the results with different cutoffs. *Agt*, *Nrgn*, *Sparc*, *Camk2n1*, *Slc17a7*, *Slc6a11* and *Tcf7l2* are at the intersection of the top 10 SVgenes identified by all methods. Among the top 500 SOMDE SVgenes, cSOMDE, SpatialDE, Giotto, scGCO and SPARK identified 435, 274, 277, 259 and 39 identical SVgenes, respectively (Supplementary Fig. S17). Compared with other methods, our method and SpatialDE use similar statistical models to infer spatial variability. Thus SOMDE has a high consistency with the results of SpatialDE.

We observed similar results in the nHipp data. SOMDE found all SVgenes identified by scGCO, and 377 SVgenes identified by SOMDE are shared with SpatialDE (Fig. 5b). Focusing on the rank similarity of the top SVgenes, we found that *Ttr*, *Mef2c*, *Pcp4*,

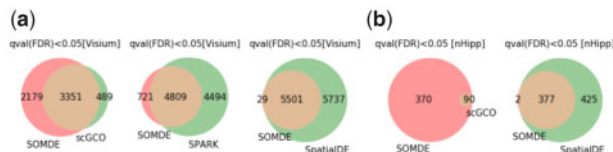


Fig. 5. Number of SVgenes identified by four methods on the 10X brain (a) and nHipp data (b). Genes with FDR (q value) < 0.05 are identified as SVgenes. Most of the 5530 genes found by SOMDE in 10X brain dataset were also identified by other methods. More than 99% SVgenes identified by SOMDE have also been identified by SpatialDE in the nHipp data. Since cSOMDE and Giotto cannot provide the SVgene number, we compared the top 500 SVgene of each method and Venn diagrams are in the [supplementary figures](#)

Pde10a, *Penk*, *Arpp21* and *Enpp2* are the intersection genes among the top 10 genes identified by SOMDE and other methods. Among the top 500 SOMDE SVgenes, cSOMDE, SpatialDE, Giotto and scGCO identified 457, 401, 277, 142 and 93 identical SVgenes, respectively ([Supplementary Fig. S18](#)). We concluded that SOMDE has a high overlap with other methods on the top SVgenes. Over half of SVgenes among the top 500 identified by SOMDE and other methods are identical, except scGCO only report 9 SVgenes in the nHipp data.

We further found that SOMDE and cSOMDE have almost identical SVgene ranks in both two datasets. They shared over 85% percent of common SVgenes cross any rank cutoffs ([Supplementary Fig. S19](#)). The diagonal rank plot ([Supplementary Fig. S19](#)) also shows that the cSOMDE result obtained from the geometric mean has a similar rank to that obtained from a single SOMDE result. Besides, we compared the SOMDE results under a set of adjacent map sizes on the 10X Brain and nHipp data ([Supplementary Fig. S20](#)). The diagonal scatter points in the rank plots elaborated that the results with adjacent map sizes (parameter k) have high similarity. We also compared the SOMDE results under different parameters γ . Similar diagonal scatter points are shown in [Supplementary Figure S21](#).

3.4.2 Running time comparison

We selected three real representative datasets: 10X Brain, nHipp and Kidney to test the computational efficiency of different methods on the large-scale data. The number of sequencing sites in these three datasets gradually increases, as shown in [Table 2](#). The comparison results of the five methods are shown in [Figure 6a](#). SOMDE spent 24, 757 and 144 s to give results in the three datasets. It took scGCO 2917, 400 and 2424 s to get the results in these datasets, although it is designed to improve the computational efficiency. Giotto and SpatialDE spent more than 5000 s on the Kidney dataset. SPARK spent more than 4 h in the 10X Brain data and failed to give the result on the nHipp data so that we did not further test it on the Kidney data. The adjustable resolution of SOM makes SOMDE the only method that gets results in large-scale datasets in 300 s. Unlike other methods, the computational complexity of SOMDE barely increases with the growth of the dataset size, and is only affected by the number of genes. Therefore, the running time in Liver and Kidney datasets is even less than which on the 10X brain data.

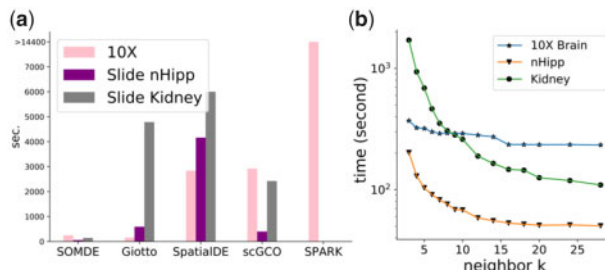


Fig. 6. Running time Comparison. (a) The total running time of five methods in three datasets with different sizes. Colors correspond to different datasets. (b) Running time of SOMDE under different neighbor numbers

To explore how the parameter k affects the running time of SOMDE, we applied SOMDE with gradually changed k on the three selected datasets and recorded the running time ([Fig. 6b](#)). From these results, we can see that a small decrease in the size of condensed map can lead to a significant improvement in the computation efficiency, as demonstrated by the sharp decrease at the beginning of the running time curves ([Fig. 6b](#)). It is also clear that the curve trends to stabilize as k gets larger enough. This is because for a large k , the condensed map becomes so small that modeling its covariance is no longer the main factor contributing to the whole running time of SOMDE.

Based on the above observations, we know that in real applications, a proper k should not be too small so that high computational efficiency can be guaranteed. Meanwhile, it should not be too large because a large k brings a small gain in the computational efficiency but a high risk of losing more local spatial patterns in the condensed map. We recommend $k = 5-20$ in SOMDE for most scenarios.

4 Discussion

The increasing throughput of spatial transcriptomic data enables researchers to study the gene expression in the spatial context at a larger scale, but brings computational challenges to bioinformatic tools as well. We present SOMDE, an SVgenes identification method that extends the application to the large-scale dataset by combining the advantages of machine learning and statistical models. SOMDE integrates gene expression and spatial locations to a condensed map by applying self-organizing map and identifies gene spatial expression variability via Gaussian Process.

The results of the simulation experiments show that SOMDE gave similar performance to SpatialDE in most cases. On high sparse data, the performance of SOMDE was better than other methods. Experiments on multiple datasets with different sequencing protocols showed that the SOM-based condensed map well preserved the topological structure and the gene spatial expression patterns. The SVgenes identified by SOMDE are highly consistent with other methods and existing gene ISH data. SOMDE also enhances the spatial patterns of SVgene expressions, which helps for better visualization. Experiments showed that choices on the condensed map size within a proper range do not change the identification results much. Therefore one SOMDE model can work for many scenarios.

It should be noted that the degree of spatial variation of a gene's expression is a relative matter and defining the hard cutoff of SVgene and non-SVgene is not feasible. This is especially true when we consider different possible modes, scales and localization of the variation. The observed null distribution of test P -values for permuted data ([Supplementary Figs S22 and S23](#)) also confirms the intrinsic complexity of this problem. This is a topic that needs further research, which should be put into the context of downstream biological analyses of the spatial variations. SOMDE provides a relative ranking of SVgenes with regard to the strength and significance of the variation.

Compared with existing methods, SOMDE is more similar to those statistical models. This is related to our choice of the Gaussian Process as the significance test model. The self-organizing map can be considered as the frontend and Gaussian process as the backend of SOMDE. The backend statistical model can take any other forms such as the marked point process used in Trendsseek or GLSM used in SPARK. SOMDE can also be extended to 3D spatial sequencing data in the future, since the Gaussian Process and SOM have no restriction on dimensionality.

A key challenge in identifying SVgenes in large-scale spatial transcriptomics data is the high computational complexity. SOMDE tackles this challenge by building a condensed map from the original data. We should notice that this also introduces limitations on the application of the method. Although SOM provides adaptive down-sampling that can better preserve the topology and densities in the original data than uniform downsampling, some local details can still be missed ([Supplementary Fig. S24](#)). We may adopt a hierarchical strategy to first detect variations at the global view first and

then at scan for local variations in smaller areas of interest to better capture SVgenes at multiple resolutions.

Acknowledgements

The authors thank Prof. Guocheng Yuan, Dr. Qian Zhu and Dr. Ruben Dries for their helpful discussions. They thank the anonymous reviewers for their constructive suggestions.

Funding

This work was supported by the National Natural Science Foundation of China (NSFC) Projects [61721003, 62050178] and National Key R&D Program of China [2018YFC0910401].

Conflict of Interest: none declared.

Data availability

The 10X Visium data (v1.0.0) can be downloaded from the official website: <https://www.10xgenomics.com/resources/datasets>. The pre-filtered slide-seq data can be downloaded from SpatialDB website: <http://www.spatialomics.org/SpatialDB/>.

References

- Dries,R. et al. (2021) Giotto: a toolbox for integrative analysis and visualization of spatial expression data. *Genome Biol.*, **22**, 78–78.
- Edsgård,D. et al. (2018) Identification of spatial expression trends in single-cell gene expression data. *Nat. Methods*, **15**, 339–342.
- Eng,C.-H.L. et al. (2019) Transcriptome-scale super-resolved imaging in tissues by RNA seqFISH. *Nature*, **568**, 235–239.
- Fan,Z. et al. (2019) SpatialDB: a database for spatially resolved transcriptomes. *Nucleic Acids Res.*, **48**, 2019.
- Kohonen,T. (1984) *Self Organization and Associative Memory*. Springer, New York.
- Lein,E.S. et al. (2007) Genome-wide atlas of gene expression in the adult mouse brain. *Nature*, **445**, 168–176.
- Ling,K.H. et al. (2011) Spatiotemporal regulation of multiple overlapping sense and novel natural antisense transcripts at the Nrgn and Camk2n1 gene loci during mouse cerebral corticogenesis. *Cerebral Cortex*, **21**, 683–697.
- Moffitt,J.R. et al. (2018) Molecular, spatial, and functional single-cell profiling of the hypothalamic preoptic region. *Science*, **362**, eaau5324. no.
- Rodrigues,S.G. et al. (2019) Slide-seq: a scalable technology for measuring genome-wide expression at high spatial resolution. *Science*, **363**, 1463–1467.
- Smith,C.M. et al. (2019) The mouse Gene Expression Database (GXD): 2019 update. *Nucleic Acids Res.*, **47**, D774–D779.
- Ståhl,P.L. et al. (2016) Visualization and analysis of gene expression in tissue sections by spatial transcriptomics. *Science*, **353**, 78–82.
- Sun,S. et al. (2020) Statistical analysis of spatial expression patterns for spatially resolved transcriptomic studies. *Nat. Methods*, **17**, 193–200.
- Svensson,V. et al. (2018) SpatialDE: identification of spatially variable genes. *Nat. Methods*, **15**, 343–346.
- Uriarte,E. et al. (2005) Topology preservation in som. *Int. J. Appl. Math. Comput. Sci.*, **1**, 19–22.
- Wittek,P. et al. (2017) Somoclu: an efficient parallel library for self-organizing maps. *J. Stat. Softw.*, **78**, 1–21.
- Zhang,K. et al. (2018) Identification of spatially variable genes with graph cuts. *BioRxiv*, **2018**, 491472.
- Zhang,X. and Li,Y. (1993) Self-organizing map as a new method for clustering and data analysis. In *Proceedings of 1993 International Conference on Neural Networks (IJCNN-93-Nagoya, Japan)*, Vol. 3, pp. 2448–2451.